Energy, Mines and Resources Canada | Energie, Mines et Ressources Canada

CANMET

Canada Centre for Mineral and Energy Technology | Centre canadien de la technologie des minéraux et de l'énergie

EFFECTS OF SINTERING CONDITIONS ON THE PHYSICAL AND CHEMICAL CHARACTERISTICS OF SEPT-ILES IRON ORE PELLETS

D.H.H. Quon and K.E. Bell
Mineral Processing Laboratory

May 1983

Project MRP-3.4.0.0.03
Iron Ore Processing

This document is an unedited internal report prepared primarily for discussion and limited distribution purposes. It does not represent a final expression of the opinion of the Canada Centre for Mineral and Energy Technology (CANMET)

Ce document est un rapport préliminaire non révisé et rédigé principalement en vue d'une diffusion limitée et de discussions. Il ne représente pas une expression définitive de l'opinion du Centre canadien de la technologie des minéraux et de l'énergie (CANMET)

MICROMEDIA

JUL 29 1983

40 pp

MINERALS RESEARCH PROGRAM
MINERAL SCIENCES LABORATORIES
DIVISION REPORT MRP/MSL 83-57 (IR)

EFFECTS OF SINTERING CONDITIONS ON THE PHYSICAL AND CHEMICAL CHARACTERISTICS OF SEPT-ILES IRON ORE PELLETS

by

D.H.H. Quon* and K.E. Bell**

ABSTRACT

This paper discusses the physical and chemical characteristics of Sept-Iles green pellets sintered under various temperatures and soak times. Particular reference is made to the crushing strength of the sintered pellets with respect to the conditions of sintering.

The results show that a preheating treatment of the green pellets prior to their use for sintering is necessary in order to reduce the defects which may be introduced into the pellets as a result of the loss of structural water, and other volatiles present in the pellets. Two of the most important parameters that affect the induration of the green pellets, viz., temperature and time, are assessed in terms of crushing strength, internal pellet structure and commonly-used pellet quality criteria.

---

*Research Scientist and **Head, Ceramic Section, Mineral Processing Laboratory, Mineral Sciences Laboratories, CANMET, EMR, Ottawa.

CARACTÉRISTIQUES PHYSIQUES ET CHIMIQUES DES AGGLOMÉRÉS DE MINERAI DE FER DE SEPT-ILES APRÈS LES AVOIR SOUMIS À DES CONDITIONS DE FRITTAGE

par

D.H.H. Quon* et K.E. Bell**

RÉSUMÉ

On discute des caractéristiques physiques et chimiques des agglomérés verts de Sept-Iles selon différentes températures et différents temps de trempe. On porte une attention spéciale à la résistance au broyage des agglomérés obtenus par frittage selon les conditions d'agglomération par frittage utilisées.

Les résultats indiquent qu'il est nécessaire de pré-traiter à la chaleur les agglomérés verts avant de les utiliser si l'on veut réduire les défauts qui peuvent être causés par la perte d'eau de structure et par la présence d'autres volatiles dans les agglomérés. On évalue deux des paramètres les plus importants qui affectent le durcissement des agglomérés verts, à savoir la température et le temps, en terme de la résistance au broyage, de la structure interne des agglomérés et de critères généralement utilisés pour évaluer la qualité des agglomérés.

---

*Chercheur scientifique et **Chef, Section de céramiques, Laboratoires de traitement des minéraux, Laboratoires des sciences minérales, CANMET, EMR, Ottawa.

CONTENTS

	Page
ABSTRACT	i
INTRODUCTION	1
EXPERIMENTAL	1
Sintering	2
Characterization of the Sintering Process	3
RESULTS AND DISCUSSION	3
Effect of Sintering Temperature and Time on the Physical and Chemical Characteristics of the Pellets	4
Physical and chemical characteristics of pellets indurated in furnace A	4
Reproducibility of the crushing strength for pellets sintered in furnace B	7
Physical and chemical characteristics of pellets indurated in furnace C	7
CONCLUSIONS	9
ACKNOWLEDGEMENTS	9
REFERENCES	10

TABLES

No.		
1.	Chemical analyses of iron ore concentrates and green pellets calcined at 600°C	11
2.	Heating and cooling rates of furnace A	12
3.	Crushing strength of pellets sintered under different conditions	13
4.	Sintering conditions, density, apparent porosity and crushing strength of pellets	14
5.	Crushing strength of pellets heat treated at 600°C, followed by sintering at different temperatures for 20 minutes	15

Page

6. Sintering conditions, crushing strength, standard deviation, maximum and minimum crushing strength for pellets sintered in furnace B 16
7. Average crushing strength for pellets sintered at 1335°C for different soak times 17

FIGURES

No.
1. Typical heating and cooling profile for furnace A 18
2. Typical heating and cooling profile for furnace B 18
3. Typical heating and cooling profile for furnace C under equilibrium mode 19
4. Typical heating and cooling profile for furnace C under non-equilibrium mode 19
5. Shrinkage and expansion of pellets versus temperature 20
6. Crushing strength of pellets sintered at various temperatures for 20 minutes 20
7. Crushing strength versus sintering temperature and time 21
8. Microstructure of pellet sintered at 1125°C for 20 min 21
9. Microstructure of pellet sintered at 1150°C for 20 min 22
10. Microstructure of pellet sintered at 1175°C for 20 min 22
11. Microstructure of pellet sintered at 1200°C for 20 min 23
12. Microstructure of pellet sintered at 1225°C for 20 min 23
13. Microstructure of pellet sintered at 1280°C for 10 min 24
14. Microstructure of pellet sintered at 1280°C for 50 min 24
15. Microstructure of pellet sintered at 1290°C for 10 min 25
16. Microstructure of pellet sintered at 1290°C for 20 min 25
17. Microstructure of pellet sintered at 1300°C for 20 min 26
18. Microstructure of pellet sintered at 1315°C for 20 min 26
19. Microstructure of pellet sintered at 1320°C for 20 min 27
20. Microstructure of pellet sintered at 1325°C for 20 min 27
21. Microstructure of pellet sintered at 1325°C for 40 min 28

Page

22. Microstructure of pellet sintered at 1345°C for 10 min 28
23. Microstructure of pellet sintered at 1345°C for 20 min 29
24. Microstructure of commercial pellet from Sept-Iles 29
25. Microstructure of pellet sintered at 1345°C for 20 min 30
26. Microstructure of pellet sintered at 1345°C for 30 min 30
27. Microstructure of pellet sintered at 1345°C for 40 min 31
28. SEM micrograph of commercial pellet from Sept-Iles 31
29. Map of Ca distribution of the Sept-Iles pellet 32
30. Map of Si distribution of the Sept-Iles pellet 32
31. SEM micrograph of pellet sintered at 1300°C for 20 min 33
32. Map of Ca distribution of the sintered pellet 33
33. Map of Si distribution of the sintered pellet 34

INTRODUCTION

An earlier investigation of the microstructure and crushing strength of sintered iron ore pellets supplied by the Iron Ore Company of Canada showed the influence of microstructural development on the crushing strength (1). The crushing strength of the Sept-Iles pellets has a mean value of 1613 N with a standard deviation of 466 N whereas the pellet quality requirements throughout the world have become more stringent, in particular with respect to the crushing strength that must be attained to meet typical sales specifications (1960 N). The poor crushing strength of the pellets has been attributed to the poorly developed bonding characteristics of the grains in the pellet. It was recognized from the previous work that the pellet strength is in part dependent on the density displayed by the microstructure. The mechanism of induration of the Sept-Iles iron ore pellets has been discussed in a previous report (1). In general two types of bonding characteristics have been observed: (a) low temperature induration (below 1300°C) shows the hematite grains bonded together by continuous and discontinuous grain growth, and (b) high temperature induration (above 1300°C) shows the hematite grains similarly bonded together with additional bonding attributable to the presence of a liquid phase. Based on the above observations, it appears that the dominant factors controlling the strength and bonding characteristics of the pellets are the sintering temperature and time.

As part of the continued program in CANMET on iron ore processing, this work is conducted to determine the optimum temperature and time of sintering of the green pellets supplied by the Iron Ore Company of Canada.

EXPERIMENTAL

The raw materials used for this study have been described by Quon and Bell (1). The as-received iron ore green pellets originated from the Sept-Iles pelletizing plant. The green pellets contained mainly hematite with a trace of quartz and carbonates. The moisture content of the green pellets varied from 7 to 8 mass %.

The as-received green pellets were first oven-dried at 125°C to remove the absorbed water and/or heat-treated to 600°C to dehydroxylate the structural water present in the goethite. Following the low temperature

heat treatment, the dried green pellets were then used for the sintering studies.

SINTERING

Sintering of the dried pellets was conducted in three different types of resistively heated furnaces. Attempts were made to duplicate the sintering conditions of the industrial process, however this was not possible due to the constraint of the furnaces available. As a result the bulk of experimental work was concentrated in determining the effect of variables such as temperature and time of sintering affecting the bonding characteristics and crushing strength of the iron ore pellets.

In brief, the three different types of furnaces used for the study are as follows:

Furnace A is a tube furnace capable of reaching a maximum temperature of 1500°C and has a uniform hot zone of 30 cm. The tube diameter is about 4 cm. Typical heating and cooling conditions used for the sintering work are shown in Fig. 1.

Furnace B is a box furnace having dimensions of 16 x 16 x 40 cm, which was employed for large-batch sintering. The disadvantage of this furnace is its slow heating and cooling rate. Typical heating and cooling rates of the furnace are shown in Fig. 2.

Furnace C is a tube furnace similar to furnace A but with a much steeper temperature gradient: it has a uniform central hot zone of approximately 8 cm surrounded on both sides by zones of lower temperature. The presence of two different temperature zones at above 1280°C was utilized as a two-step sintering process. The dried pellets were first introduced into the furnace at the low temperature zone, approximately 1015°C, as a presintering step for the decomposition of the carbonates, and the final sintering of the pellets was conducted in the hot zone of the furnace. Typical heating and cooling profiles of this furnace are given in Fig. 3 and 4. The profile in Fig. 3 is designated as the equilibrium sintering temperature condition, whereas the profile in Fig. 4 is designated as the non-equilibrium sintering condition.

CHARACTERIZATION OF THE SINTERING PROCESS

The techniques used to characterize the raw materials and sintered pellets are as follows:

(a) Chemical analysis - both iron ore concentrates and green pellets after calcining to 600°C were analyzed and their chemical compositions are given in Table 1.

(b) Crushing strength - the crushing strength of the sintered pellets was determined using a Seger tester*. The compression tests were conducted according to testing procedures proposed by ISO (2).

(c) Heating microscopy - a Leitz heating microscope was used to determine the effect of heating on the shrinkage of the dried pellets and their sintering behaviour.

(d) X-ray diffraction analysis (XRD) - the phases present in the sintered pellets were determined using a Guinier-deWolf camera.

(e) Density and apparent porosity - both density and apparent porosity of pellets sintered under various conditions were determined. The density of the pellets was calculated from their mass and volume using a mercury displacement apparatus**. The apparent porosity of the pellets was determined according to ASTM C67-66.

(f) Optical and scanning electron microscopy - polished sections of the sintered pellets were prepared. The microstructures of the pellets were examined using either optical (OM) or scanning electron (SEM) microscopy. Qualitative determinations of Ca and Si in the pellets were obtained using energy dispersive X-ray (EDXR).

RESULTS AND DISCUSSION

The mineralogy of the green pellets was examined by XRD. The various phases detected were hematite, goethite, quartz, feldspar, calcite and clay minerals (bentonite).

---

* Manufactured by Chem. Lab., Fur Tonindustrie, Kom Ges, Berlin-West

** Amster volumeter, type VM9, manufactured by Alfred J. Amster & Co., Schaffausen, Switzerland

The physical and chemical changes of the green pellets with temperature were examined using a Leitz heating microscope. An oven-dried green pellet was used for this study, and the temperature range from 200 to 1450°C was investigated. The shrinkage and expansion of the pellet due to heating was determined as described in a previous report (1). Figure 5 is a plot of shrinkage of the green pellet and shows that shrinkage occurred at 550, 1000 and 1450°C. The shrinkage at 550°C is attributed to the dehydroxylation of the goethite and that at 1000°C is due to the decomposition of the carbonates present in the pellet. The high temperature shrinkage is due to the reduction of hematite to magnetite.

EFFECT OF SINTERING TEMPERATURE AND TIME ON THE PHYSICAL AND CHEMICAL CHARACTERISTICS OF THE PELLETS

As already mentioned earlier, the physical development of the sintered pellets relates directly to the conditions of the heat treatment. Parameters such as heating and cooling rates, and temperature and time of sintering have a great influence on the physical characteristics of the pellets. It is to be expected that pellets indurated under different sintering conditions would produce a difference in physical and chemical characteristics. As the green pellets were indurated in three different furnaces, with four different heating and cooling profiles, it is therefore appropriate to discuss the physical and chemical characteristics of the pellets indurated under different conditions.

Physical and Chemical Characteristics of Pellets Indurated in Furnace A

The green pellets used for induration in furnace A were oven-dried at 125°C. Typical heating and cooling rates of this furnace are given in Fig. 1. The green pellets were loaded into the furnace at 900°C for 5 minutes to decompose the carbonates in the pellets. Following the decomposition, they were loaded into the sintering zone under conditions given in Table 2. Upon completion of sintering, the pellets were allowed to cool to 900°C prior to their removal from the furnace. After the pellets were removed from the furnace, they were covered with mineral fibres to prevent induced thermal shock. After the pellets cooled to room temperature, they were tested in compression as well as examined by optical microscopy to determine their microstructural changes.

The crushing strength of the pellets versus sintering temperature and time are given in Table 3. The results show a general increase in crushing strength with increased sintering temperature and time. The poor reproducibility of the crushing strength under each sintering condition indicates that the original structure of green pellets used for the sintering studies may not be as uniform as anticipated.

The effect of sintering temperature at a constant soak time of 20 minutes on the physical and chemical characteristics of the pellets was investigated. Figure 6 shows a plot of crushing strength versus sintering temperature of the pellets, which confirmed the earlier finding that pellet strength increases with increasing sintering temperature. The results also show that an acceptable crushing strength of the pellets can be obtained by sintering at a temperature of 1320°C for 20 minutes. The effect of sintering time at constant sintering temperatures of 1280, 1300, 1325 and 1345°C on the crushing strength development of the pellets was investigated. The results obtained are plotted in Fig. 7 and indicate that the crushing strength of the pellets improved with an increase in sintering time.

Microstructural development of the pellets with respect to both sintering temperature and time was examined by optical microscopy. Typical microstructures of the sintered pellets are shown in Fig. 8 to 23. The pellets sintered at temperatures from 1125 to 1290°C for 10 to 20 minutes have microstructures fairly similar to those of the commercial pellets from Sept-Iles (Fig. 24). Under the above sintering conditions the hematite grains in the pellet are bonded together by continuous and discontinuous grain growth with numerous pores being formed at the grain boundaries. Microstructures of the pellets sintered above 1300°C show the hematite grains being modified. Particularly noticeable is the rounding of the grains due to the presence of a liquid phase, indicating that solution and precipitation probably occurred, with some of the hematite grains being dissolved by the liquid and reprecipitated at the grain boundaries. Sintering conducted at high temperatures indicates that the grains are bonded together by the liquid phase.

Microstructures of the pellets sintered at a constant temperature of 1345°C from 10 to 40 minutes are shown in Fig. 25 to 27. It is evident from these figures that the grain size increases and porosity decreases with increased soak time, hence the bonding of the grains is stronger.

A SEM micrograph of a commercial pellet from Sept-Iles is given in Fig. 28; EDXR maps for Ca and Si in this sample are shown in Fig. 29 and 30 respectively. The SEM micrograph shows the hematite grains are bonded by continuous and discontinuous grain growth resulting from solid state reaction. Quartz grains were observed in the sinter as an unreacted product. In the EDXR maps, the Ca appears to concentrate in the hematite grains and the Si concentrates mainly in the unreacted quartz grains and is also dispersed in hematite grains as well as at the grain boundaries. Figure 31 is a SEM micrograph for pellets sintered under controlled laboratory conditions; EDXR maps for Ca and Si of the same sample are given in Fig. 32 and 33 respectively. The SEM micrograph shows that the grains are bonded together by a slag phase, with minor pores being trapped within the grains. The EDXR maps for Ca and Si show that these two constituents are associated with the slag phase and occur mainly at the grain boundaries of the hematite.

Both density and apparent porosity measurements were conducted on the sintered pellets. Table 4 gives the sintering conditions, crushing strength, density, and apparent porosity of the sintered pellets. The results again show that pellets with high crushing strength are high in density and low in porosity, and are obtained by sintering either at higher temperature or longer sintering time.

The effect of preheating of the green pellets prior to final sintering was investigated, based on the heating microscopy results discussed earlier. The expansion followed by shrinkage of the green pellet at a temperature of approximately 600°C was attributed to the dehydration of the goethite. During this phase transition, the structural water was trapped within the pellet and bloating occurred as the temperature increased, simultaneously forcing the grains apart and resulting in the development of inferior pellet quality. An attempt was made to correct this situation by the introduction of an additional sintering step: calcining the pellets at 600°C for 10 minutes prior to the final sintering. The crushing strength of the sintered pellets with the additional calcining stage and then sintered at various temperatures for 20 minutes is given in Table 5. The crushing strengths given in Table 5 are higher than those given in Table 3 for pellets sintered under similar conditions without the additional calcining step.

Reproducibility of the Crushing Strength for Pellets Sintered in Furnace B

In order to determine the reproducibility of the crushing strength of the pellets under different sintering conditions, furnace B was used for the experimental work. This furnace is capable of handling large batches and has a very slow heating and cooling rate (Fig. 2). It has been shown earlier that the crushing strength of the sintered pellets varies under identical sintering conditions and it was suspected that this variation was related to the quality of the original green pellets. Approximately 300 green pellets were used for this sintering study as opposed to the three or six pellets being used for the earlier experimental work. The oven-dried green pellets were sintered in furnace B at temperatures of 1250, 1300 and 1345°C for a period of 20 minutes. On completion of the sintering, 60 pellets were randomly selected for crushing. The average strength, standard deviation, maximum and minimum strength of these for pellets, sintered at different temperatures, are given in Table 6. It is readily apparent from the table that poor reproducibility of pellet strength was obtained. Apparently some of the green pellets contain some form of defects resulting in non-uniform sintered strength. The higher crushing strength of the pellets obtained in furnace B, when compared with those results obtained in furnace A, is understandable as these pellets were sintered under equilibrium conditions where all the constituents in the pellets had fully reacted, even at a sintering temperature as low as 1250°C. As this process is extremely slow and not economical, it would not be useful in commercial applications.

Physical and Chemical Characteristics of Pellets Indurated in Furnace C

It has been demonstrated earlier that the pellet strength increases with an additional calcining step at 600°C. Chemical analysis (Table 1) shows that the pellets calcined at the above temperature contained more calcium and magnesium than the sample of concentrates. These two elements appear to concentrate in the form of carbonates in the green pellets. It has been pointed out that upon heating to about 1000°C, the carbonates would decompose. During the decomposition, bloating of the pellets may occur as the CO_2 tries to escape from the interior of the pellets. This bloating is undesirable and would result in impairment of pellet quality. Based on the above assumption a further processing step was introduced into the sintering investigation. The green pellets used for this study were

either oven-dried at 125°C or heat-treated at 500°C to remove the physiosorbed or chemisorbed water. The heat-treated pellets were then loaded into the cool zone of the furnace at 1025°C for a period of 10 minutes to allow the carbonates to decompose slowly. This step was followed by loading the pellets into the sintering zone at 1335°C, using a soak period varying from 10 to 40 minutes. Upon completion of the sintering step, the pellets were removed to the lower temperature zone and, after the temperature became stabilized, they were removed from the furnace and again covered with mineral fibre to reduce possible thermal shock. The two heating and cooling profiles employed for the sintering study (shown in Fig. 3 and 4) are designated as equilibrium and non-equilibrium sintering conditions. The difference between these two modes is based on the temperature decrease owing to mass effect as the pellets were loaded into the sintering zone. In the equilibrium sintering mode there was little temperature drop, and the pellets were exposed for essentially the full soak time at the exact sintering temperature. In the non-equilibrium mode there was significant cooling, and the soak time included a period of temperature stabilization. Thus, in the equilibrium sintering mode the pellets have a longer residence time at the sintering temperature.

The crushing strength of the pellets sintered at 1335°C with varying soak time under the two different modes are given in Table 7. It can be seen that the pellet strength is higher for sinters obtained under the equilibrium mode than for those from the non-equilibrium mode. Furthermore, the crushing strength of the green pellets heat treated at 500°C is higher than the oven-dried green pellets.

The effect of soak time at a sintering temperature of 1280°C was also investigated in a similar manner. The crushing strength versus soak time is given in Table 7. It can be seen from the table that the crushing strength is higher for the pellets sintered under the equilibrium mode than for those sintered under the non-equilibrium mode, although the difference in pellet strength is less noticeable due to the preheat treatment of the green pellets.

Based on the results obtained, it is evident that all the conditions of sintering affect the pellet crushing strength. Again, it has been illustrated that the sintering temperature and time affect the strength development of the pellets. Other parameters showing less effect on the strength development of the pellets include the manner in which the green

pellets are treated prior to the sintering process, such as removal of the pelletizing and structural water, dehydroxylation of the goethite and decomposition of the carbonates prior to the sintering step.

CONCLUSIONS

It has been demonstrated that a preheat treatment of the green pellets prior to their sintering is necessary to reduce possible defects that may be introduced into the green pellets due to rapid loss of physiosorbed and chemisorbed water, dehydroxylation of goethite, and decomposition of the carbonates.

Both sintering temperature and soak time are found to be critical in controlling the strength development of the sintered pellets. The bonding mechanism in the sinter process involves the solid state reaction of the hematite grains at lower sintering temperatures. Using a lower temperature for the pellet induration, the crushing strength is lower because the bonding of the grains in the pellets is also weaker. Induration of the pellets conducted at high sintering temperatures improves the crushing strength. The grains in the pellets are bonded by a slag phase as well as both continuous and discontinuous grain growth. The soak time acts in a similar manner, i.e., a longer soak time both promotes grain growth and reduces porosity at low sintering temperatures. At high sintering temperatures and increased soak time, more slag phase is formed and hence the bonding becomes stronger. The presence of the slag phase in the sinter has a great beneficial effect on the pellet strength. This is attributed in part to the redistribution of the constituents in the iron ore concentrates from a less homogeneous to a more homogeneous body.

Pellets with adequate strength have been produced under laboratory controlled conditions.

ACKNOWLEDGEMENTS

We wish to express our gratitude to the Iron Ore Company of Canada for supplying the green pellets for this study. Thanks are also due to D. Owen for performing the scanning electron microscopy, to Y. Bourgoin for the preparation of polished sections, and to G. Lemieux for his assistance in the experimental work.

REFERENCES

1. Quon, D.H.H. and Bell, K.E. "Characterization and sintering of commercial iron ore pellets: a progress report"; Division Report MRP/MSL 81-61 (IR); CANMET, Energy, Mines and Resources Canada, 1981.

2. "Iron ore pellets - determination of crushing strength"; Third draft proposed ISO/DP 4700; ISO/TC 102/3 N 456; Jan. 12, 1979.

Table 1 - Chemical analyses of iron ore concentrates and green pellets calcined at 600°C

	Iron ore concentrates	Green pellet calcined at 600°C
Total Fe	64.6	63.8
MnO	0.51	0.51
TiO_2	0.27	0.25
SiO_2	4.10	4.65
Al_2O_3	1.36	1.46
CaO	0.01	1.11
MgO	0.50	1.15
L.O.I.	4.24	3.60

Table 2 - Heating and cooling rates of furnace A

Sintering temperature, (°C)	Temperature to reach 900°C, (min)	Time to cool from sintering temperature to 900°C, (min)
1345	60	55
1320	30	50
1300	20	40
1290	18	40
1280	19	40
1250	17	30
1200	16	30
1150	15	25

Table 3 - Crushing strength of pellets sintered under different conditions

Temp (°C)	Time (min)	Crushing strength (N)	Average strength (N)
1345	40	3166,3293,2272	2901
	30	2566,1793,1068	2143
	20	2048,2156,1234,1707,3688	2167
	10	1480,1548,1195	1528
1325	40	2569,2716,2197,1764,3724,2185	2526
	30	1842,1715,1490	1682
	20	1617,2509,1656	1927
	10	2166,1284,1235	1562
1300	40	1568,2548	2058
	30	1176,1019,1764,2098,3040,2157	1876
	20	1529,1519,1960,1451,1638,1569	1698
	10	1873,1764,1666	
1290	40	1373,906,2010,1471,2863	1724
	20	1902,1549,2197	1882
	10	1196,1617,1530,686,981	1202
1280	50	3290,2068,1764	2584
	40	1470,1470,2803	1914
	35	2195,1274,490	1320
1225	20	2481,1912,1902	2098
1200	20	1079,2275,745	1366
1175	20	981,981,1078	1013
1150	20	588,981,647	739
1125	20	588,441,745	591

Table 4 - Sintering conditions, density, apparent porosity and crushing strength of pellets

Sintering temp (°C)	Sintering time (min)	Density (kg/m^3)	Apparent porosity (%)	Crushing strength (N)
1200	20	3457	28	1340
1250	20	3560	26	1334
1275	20	3627	25	2076
1300	20	3644	24	1800
1325	20	3806	20	2144
1345	20	3850	17	2997

Table 5 - Crushing strength of pellets heat treated at 600°C, followed by sintering at different temperatures for 20 minutes

Sintering temp (°C)	Crushing strength (N)	Average crushing strength (N)
1200	1872,1765,1971	1870
1225	2393,2255,1902	2183
1250	1137,1971,2868	1334
1275	2040,2157,2030	2076
1300	2422,2589,2108	2373
1325	2648,2334,2471	2484
1345	2942,3550,2471	2988
1375	4609,2265,3069	3314

Table 6 - Sintering conditions, crushing strength*, standard deviation, maximum and minimum crushing strength for pellets sintered in furnace B

Sintering temp (°C)	Soak time (min)	Average strength (N)	Standard deviation (N)	Maximum strength (N)	Minimum strength (N)
1345	20	3561	± 980	6668	980
1300	20	3337	± 293	5099	1176
1250	20	3227	± 250	6472	1294

*Strength values obtained by averaging results for 60 pellets

Table 7 - Average crushing strength* for pellets sintered at 1335°C at different soak times

Heat treatment of green pellet	Sintering time (min)	Sintering mode (NE)	Sintering mode (E)	Average strength (N)	Standard deviation (N)
A	10		x	2728	995
A	10	x		1951	501
A	20		x	3217	1344
A	20	x		2948	1231
A	30		x	3035	693
A	30	x		2515	980
A	40		x	2559	1029
A	40	x		2324	1011
B	10	x		2113	709
B	10		x	2280	915
B	15		x	2083	929
B	15	x		1986	1093
B	20		x	2417	977
B	20	x		1794	406
B	25		x	2275	874
B	25	x		2725	1068
B	40		x	2432	1136
B	40	x		2393	690

A = green pellets heated to 500°C
B = green pellets oven-dried at 125°C
NE = non-equilibrium sintering condition
E = equilibrium sintering condition

* Average crushing strength obtained from 10 test pellets

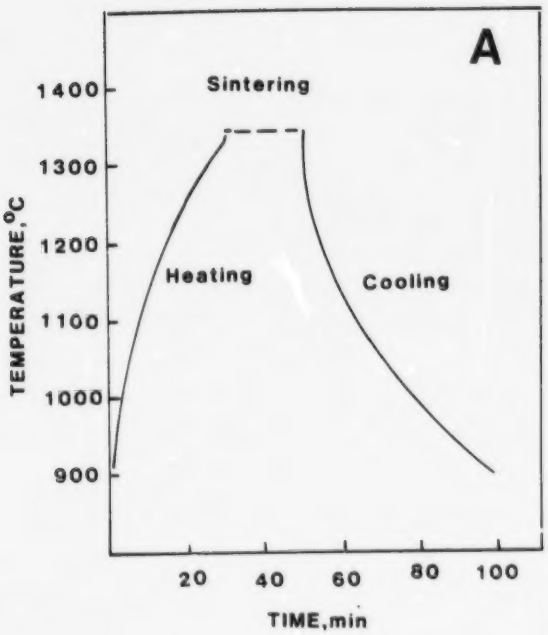

Fig. 1 - Typical heating and cooling profile for furnace A.

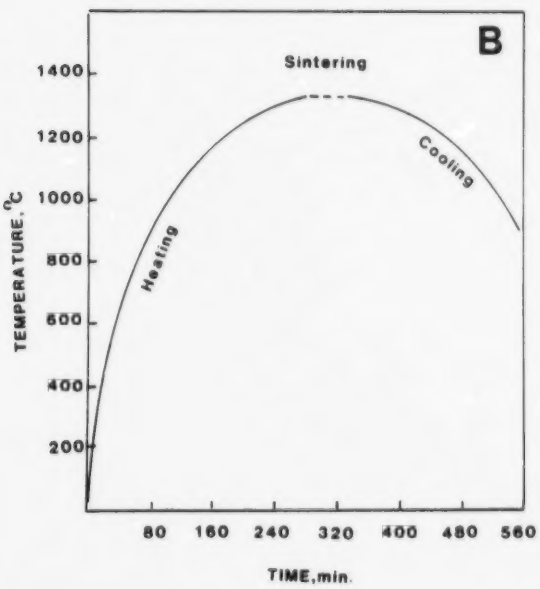

Fig. 2 - Typical heating and cooling profile for furnace B.

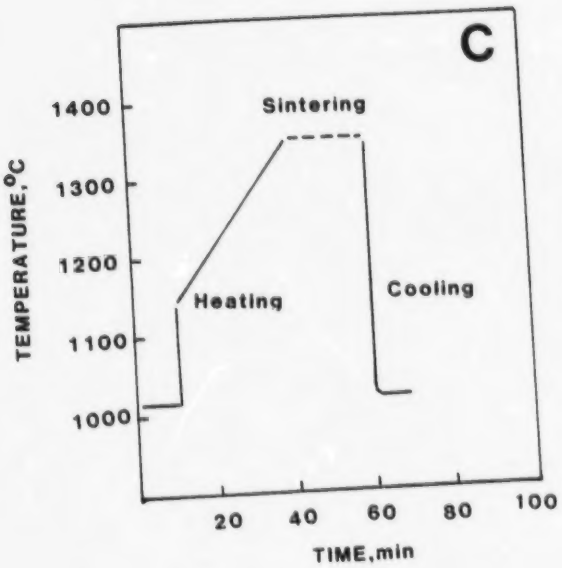

Fig. 3 - Typical heating and cooling profile for furnace C under equilibrium mode.

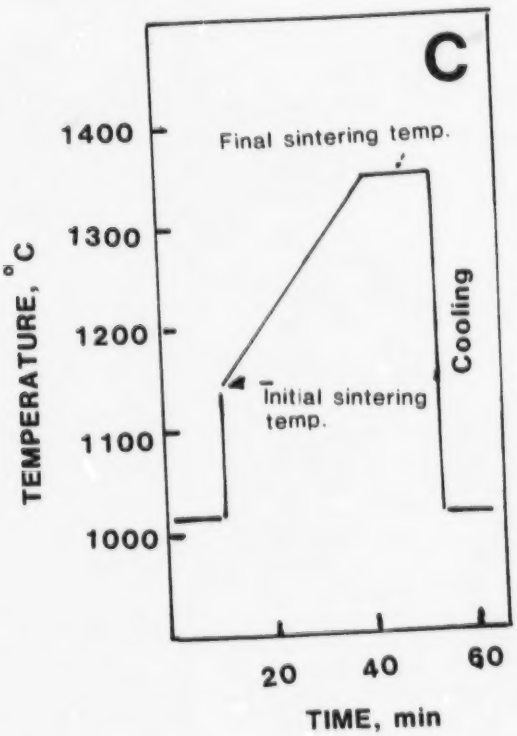

Fig. 4 - Typical heating and cooling profile for furnace C under non-equilibrium mode.

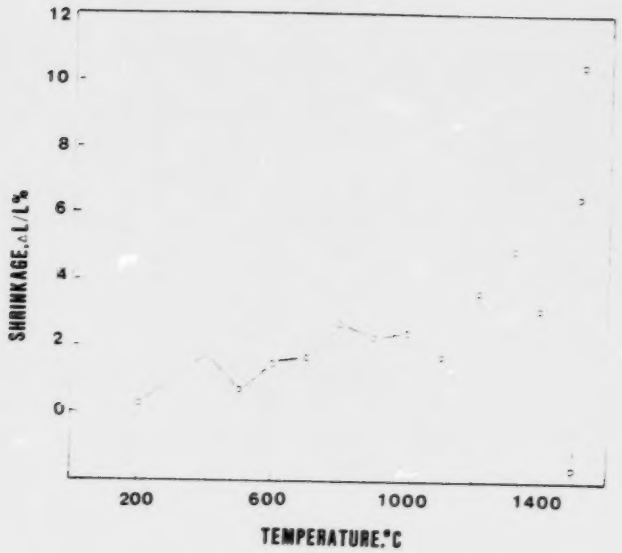

Fig. 5 - Shrinkage and expansion of pellets versus temperature.

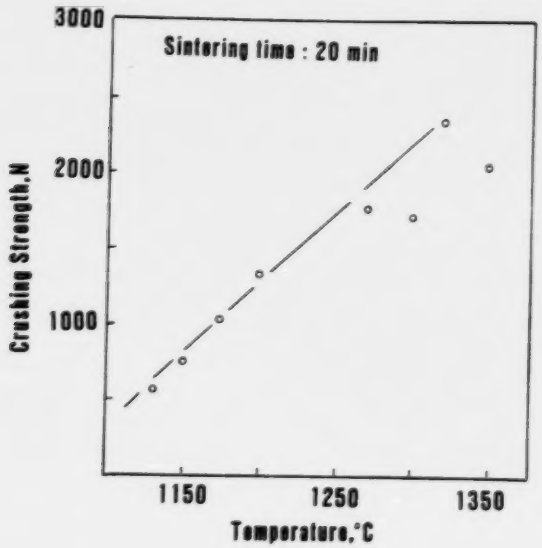

Fig. 6 - Crushing strength of pellets sintered at various temperatures for 20 min.

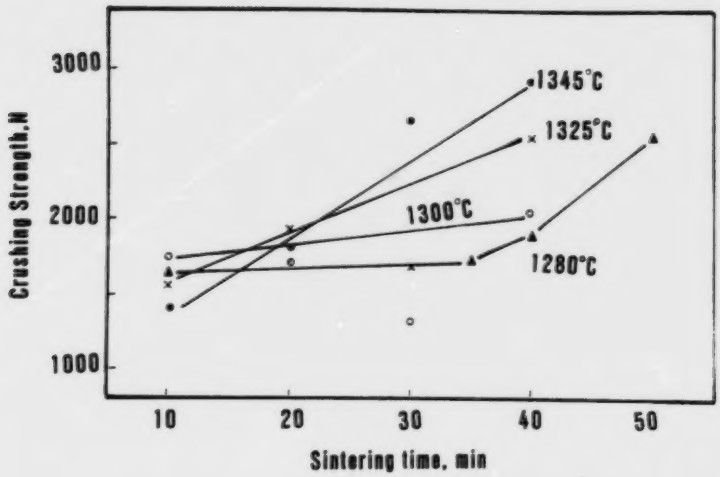

Fig. 7 - Crushing strength versus sintering temperature and time.

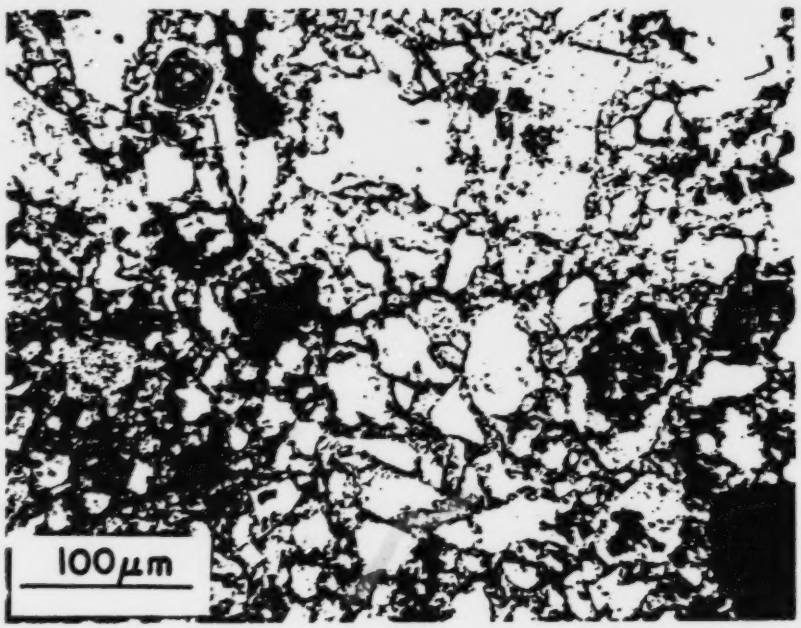

Fig. 8 - Microstructure of pellet sintered at 1125°C for 20 min.

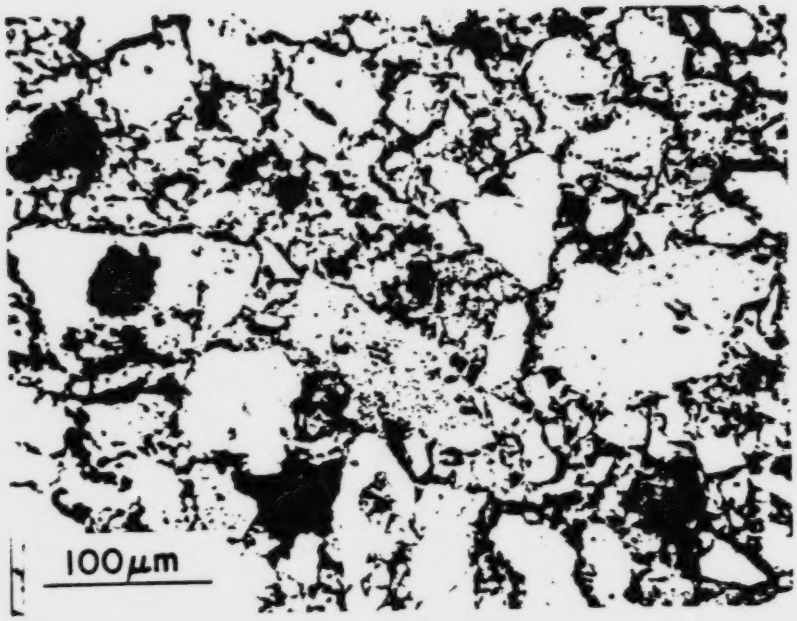

Fig. 9 - Microstructure of pellet sintered at 1150°C for 20 min.

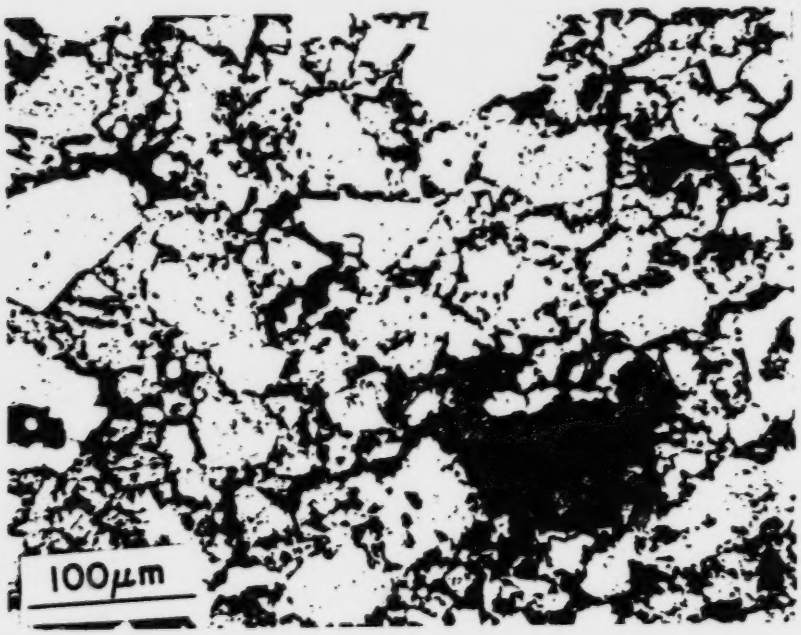

Fig. 10 - Microstructure for pellet sintered at 1175°C for 20 min.

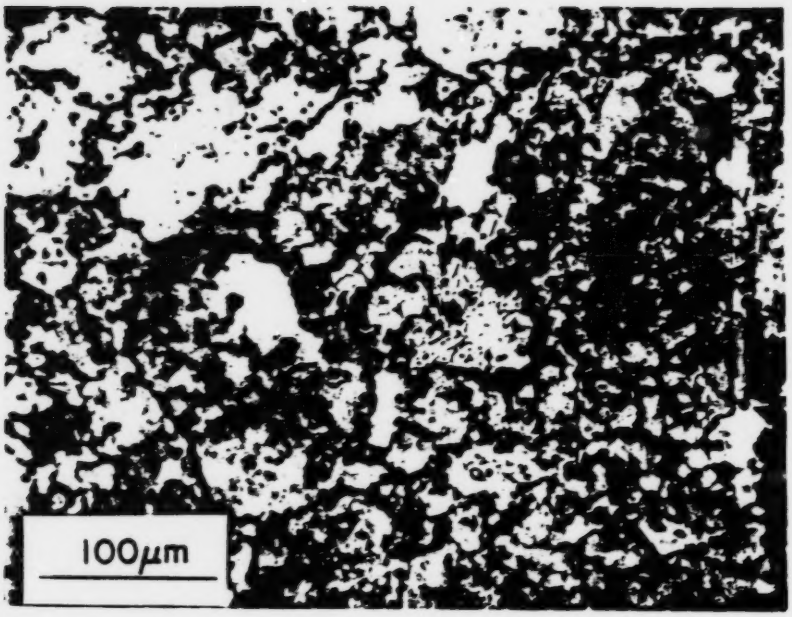

Fig. 11 - Microstructure of pellet sintered at 1200°C for 20 min.

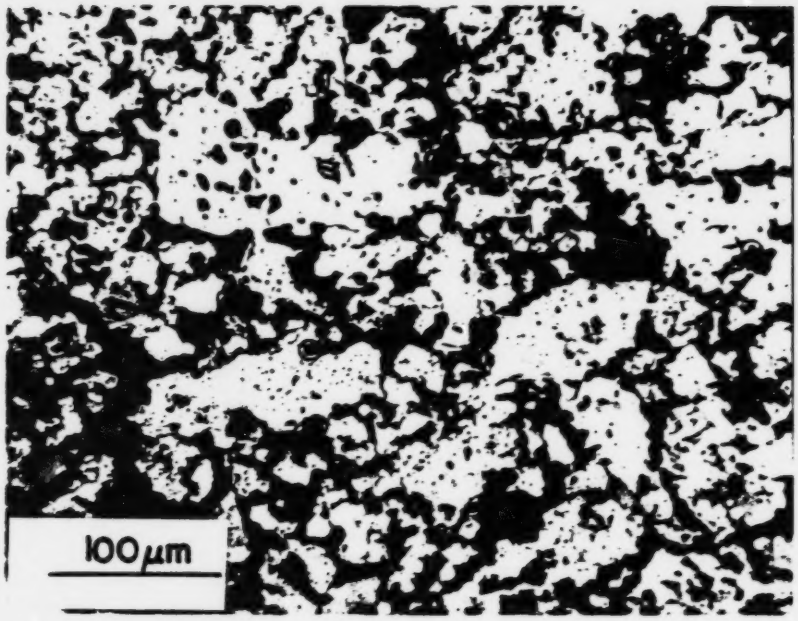

Fig. 12 - Microstructure of pellet sintered at 1225°C for 20 min.

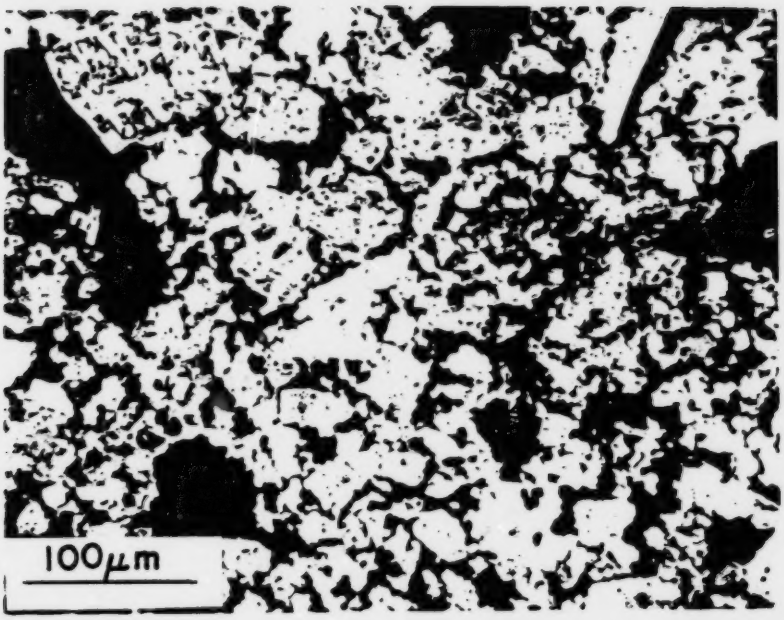

Fig. 13 - Microstructure of pellet sintered at 1280°C for 10 min.

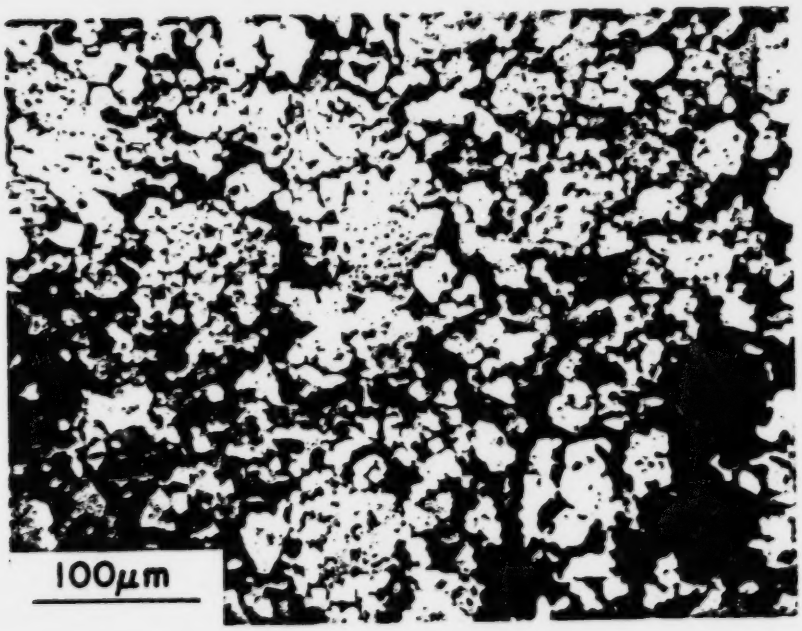

Fig. 14 - Microstructure of pellet sintered at 1280°C for 50 min.

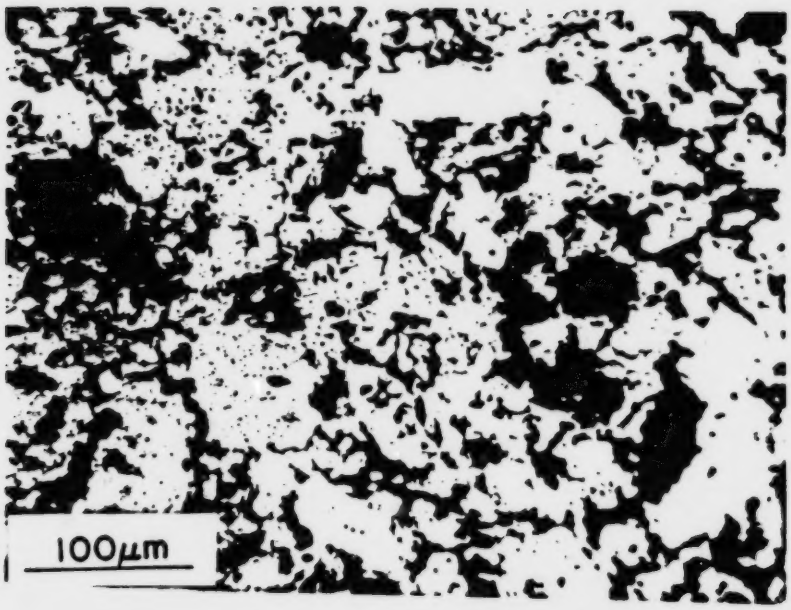

Fig. 15 - Microstructure of pellet sintered at 1290°C for 10 min.

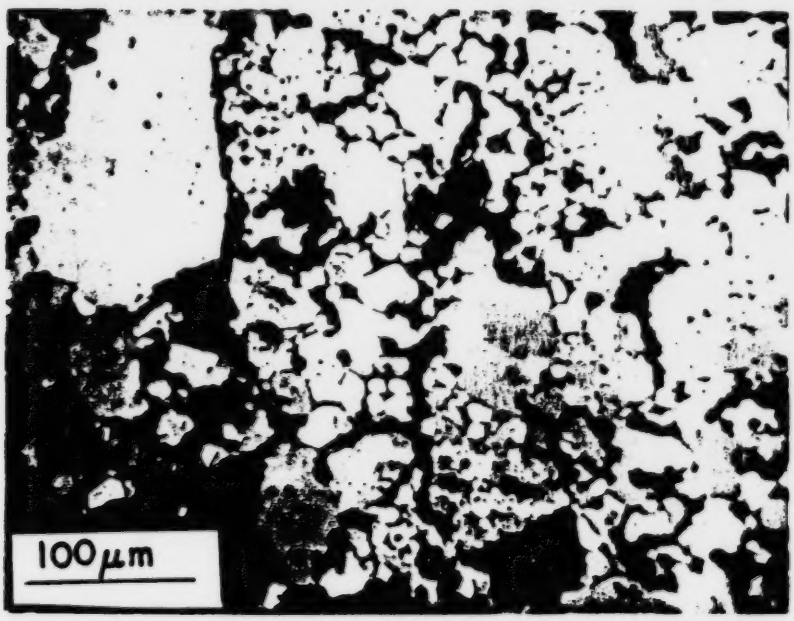

Fig. 16 - Microstructure of pellet sintered at 1290°C for 20 min.

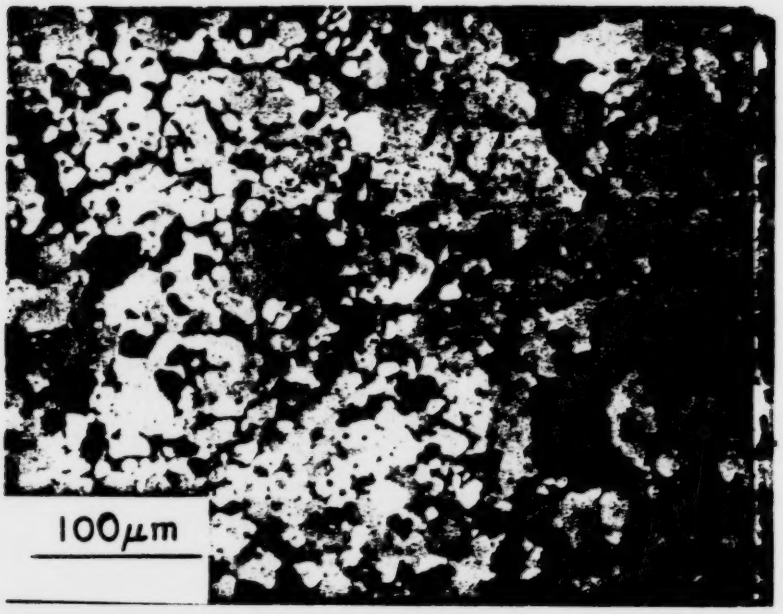

Fig. 17 - Microstructure of pellet sintered at 1300°C for 20 min.

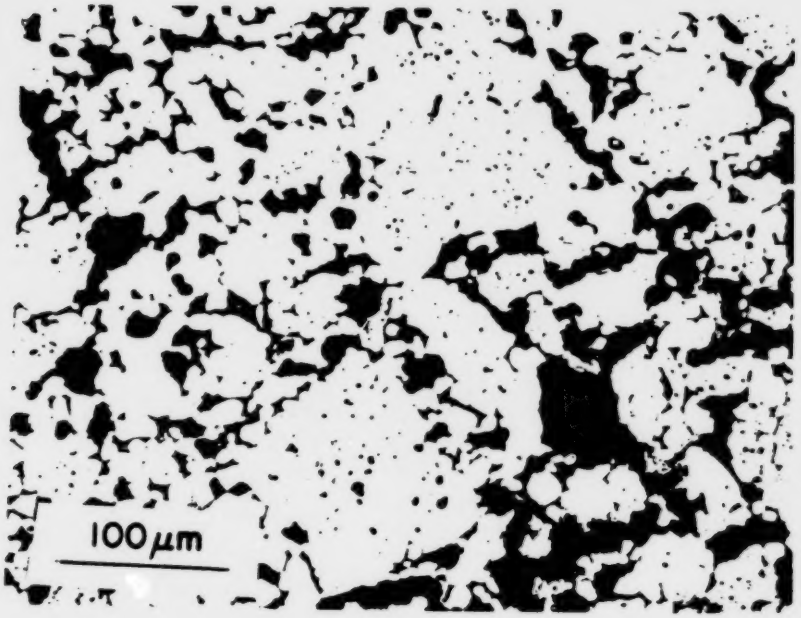

Fig. 18 - Microstructure of pellet sintered at 1315°C for 20 min.

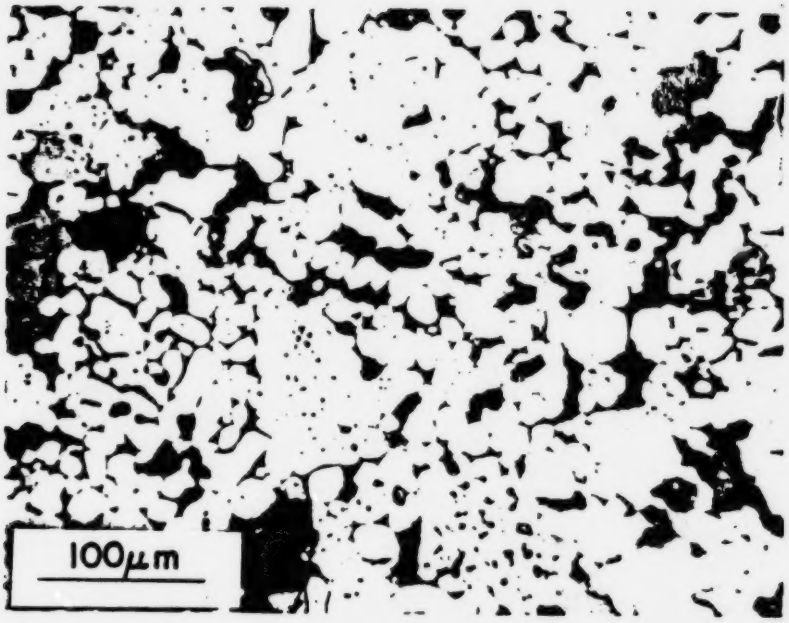

Fig. 19 - Microstructure of pellet sintered at 1320°C for 20 min.

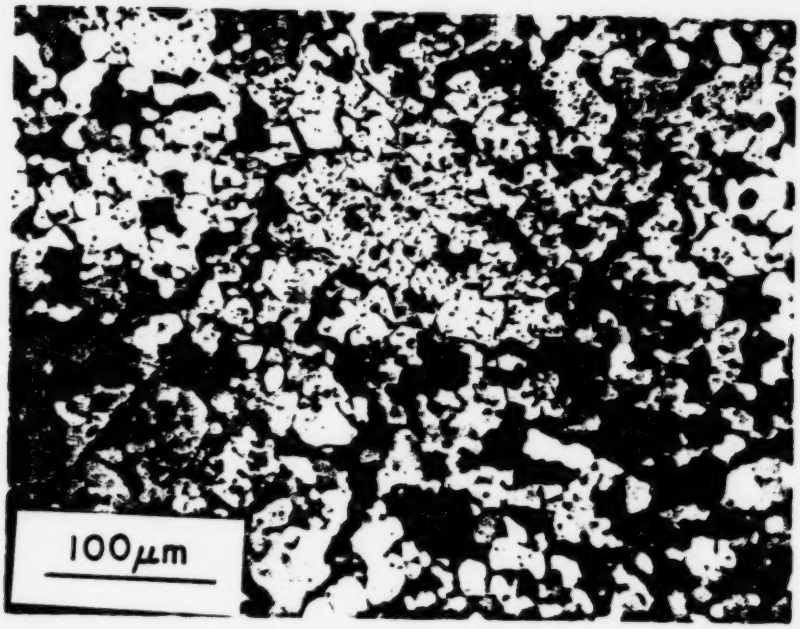

Fig. 20 - Microstructure of pellet sintered at 1325°C for 20 min.

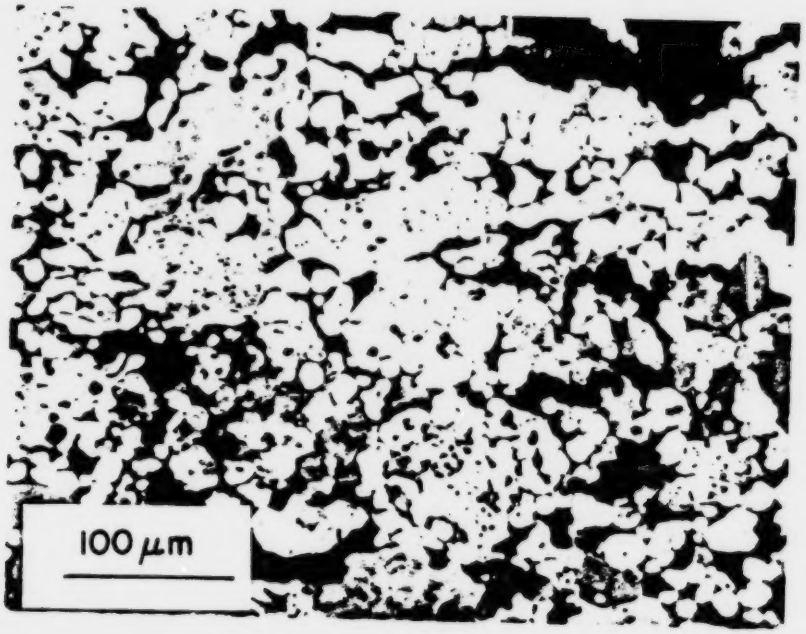

Fig. 21 - Microstructure of pellet sintered at 1325°C for 40 min.

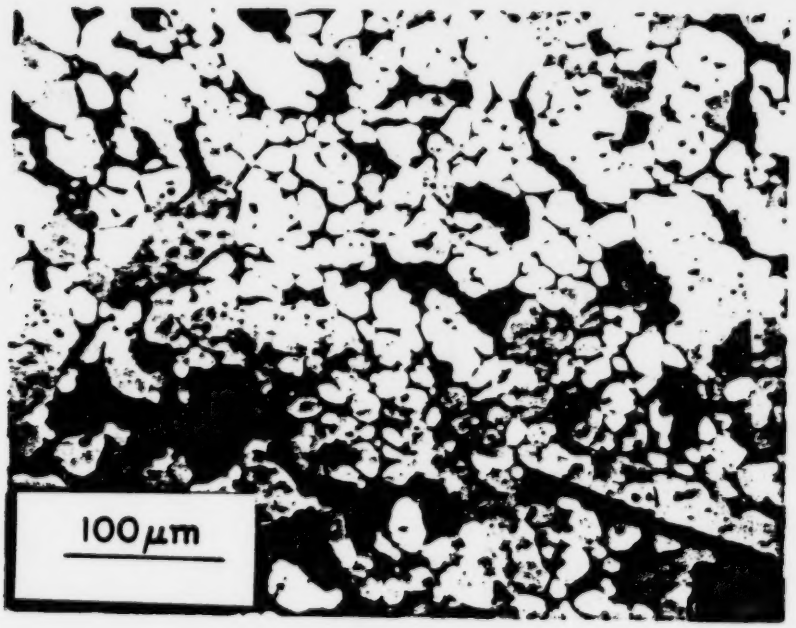

Fig. 22 - Microstructure of pellet sintered at 1345°C for 10 min.

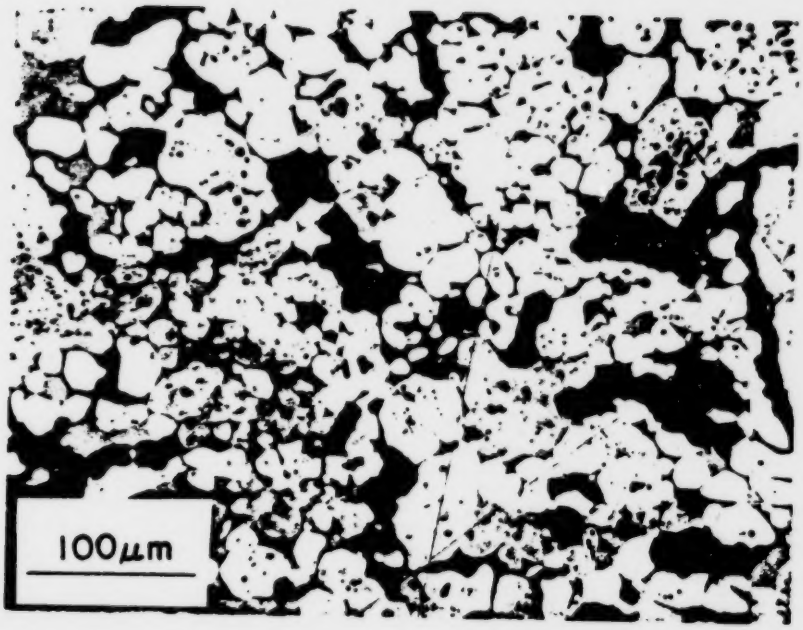

Fig. 23 - Microstructure of pellet sintered 1345°C for 20 min.

Fig. 24 - Microstructure of commercial pellet from Sept-Iles.

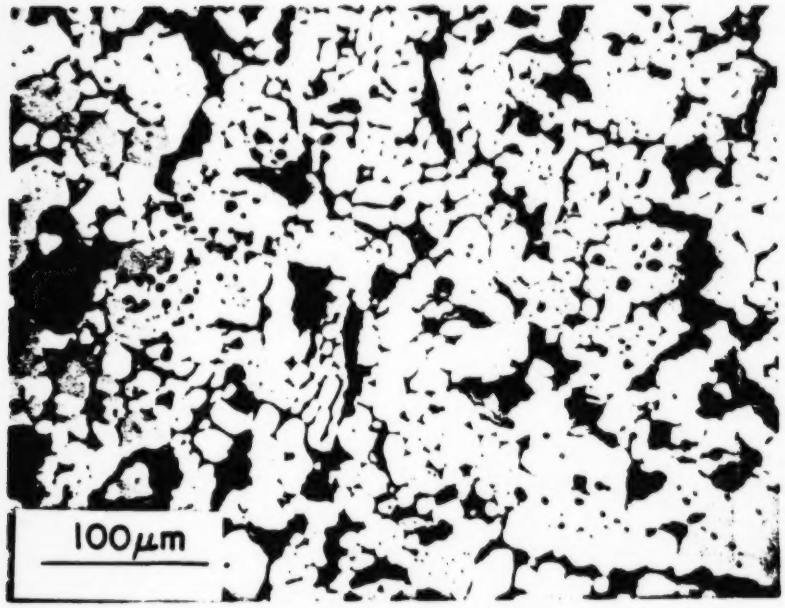

Fig. 25 - Microstructure of pellet sintered at 1345°C for 20 min.

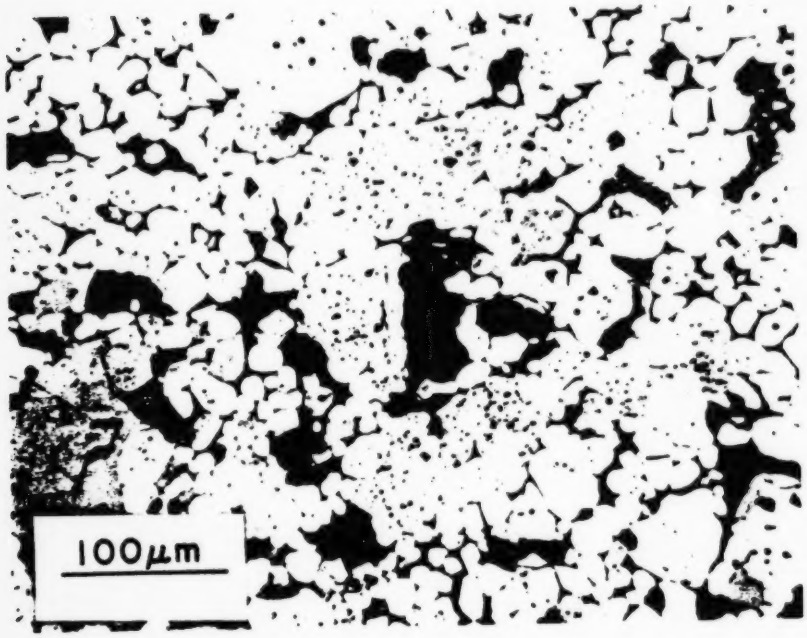

Fig. 26 - Microstructure of pellet sintered at 1345°C for 30 min.

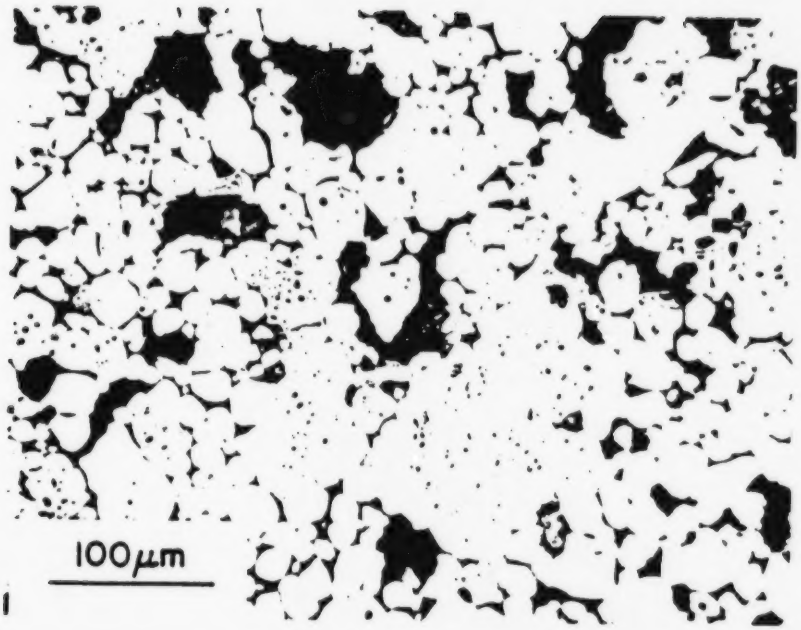

Fig. 27 - Microstructure of pellet sintered at 1345°C for 40 min.

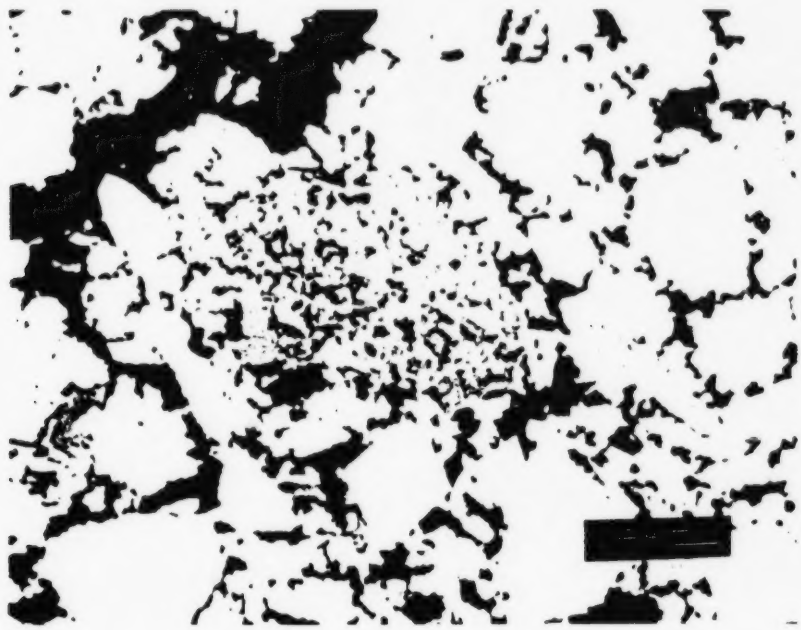

Fig. 28 - SEM micrograph of commercial pellet from Sept-Iles.

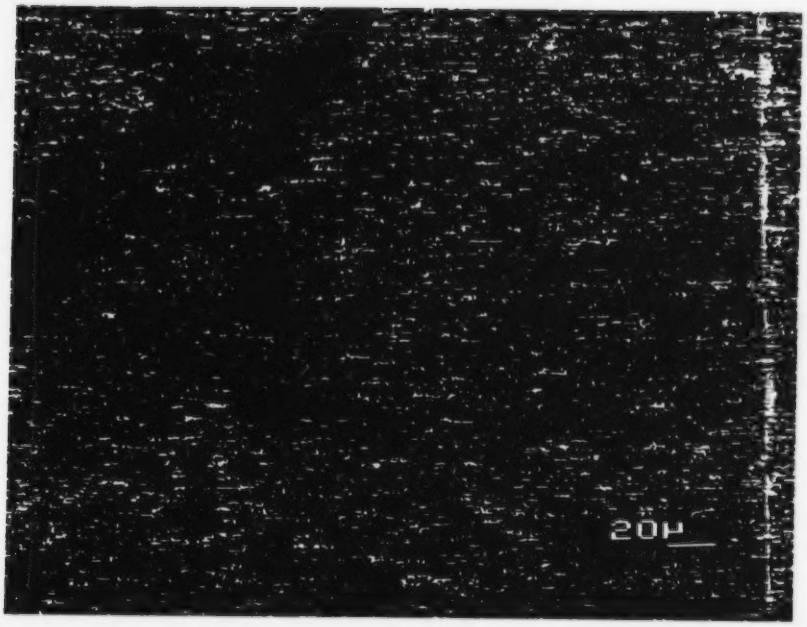

Fig. 29 - Map of Ca distribution of the Sept-Iles pellet.

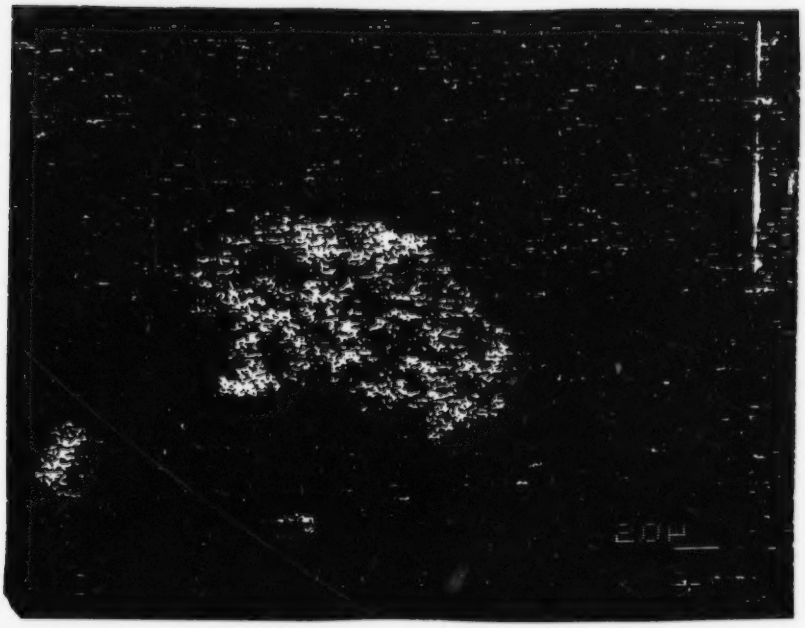

Fig. 30 - Map of Si distribution of the Sept-Iles pellet.

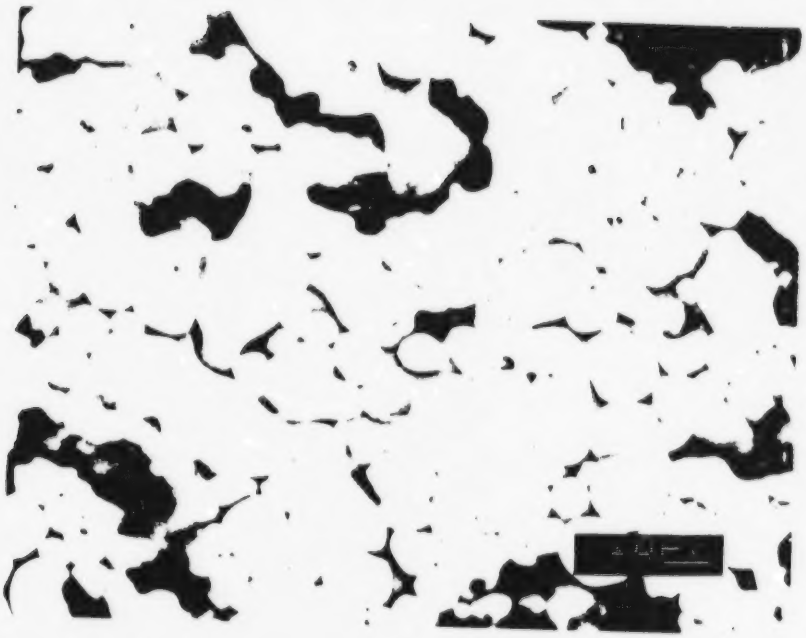

Fig. 31 - SEM micrograph of pellet sintered at 1300°C for 20 min.

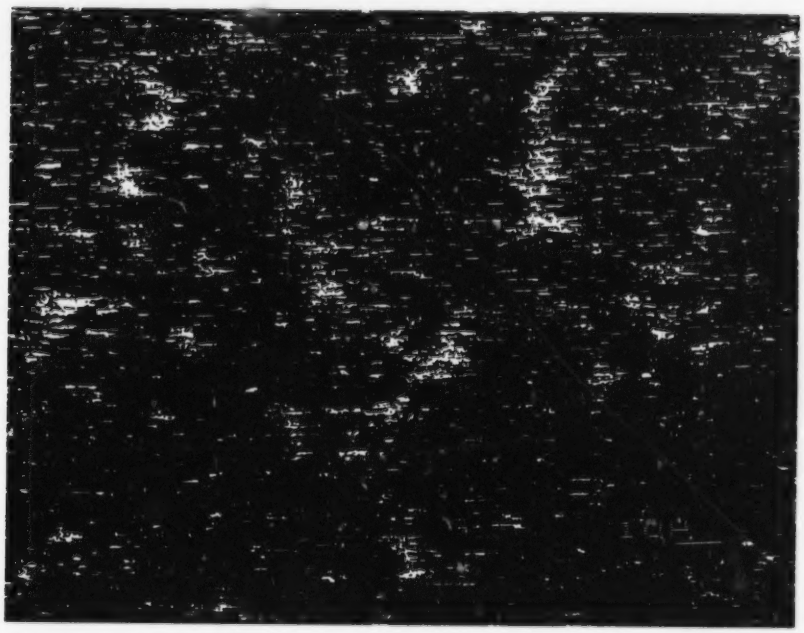

Fig. 32 - Map of Ca distribution of the sintered pellet.

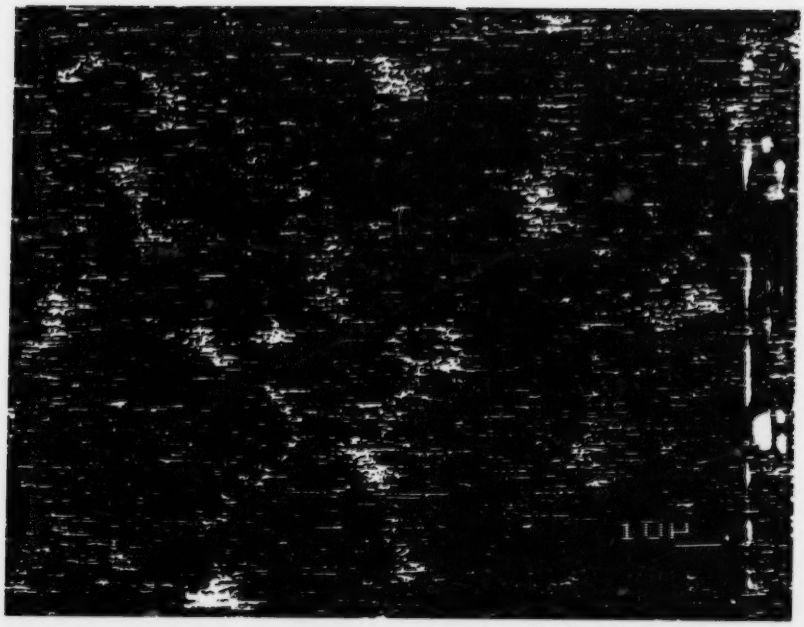

Fig. 33 - Map of Si distribution of the sintered pellet.